

Received July 7, 2020, accepted July 30, 2020, date of publication August 3, 2020, date of current version August 17, 2020.

Digital Object Identifier 10.1109/ACCESS.2020.3013932

Electromagnetic Force Distribution and Axial Deformation Uniformity Analysis of Dual-Coil Electromagnetic Tube Compression Method

LI QIU^{ID}1,3, (Member, IEEE), YUDONG WANG^{ID}1, ZHANG WANG^{ID}1, AHMED ABU-SIADA^{ID}2, (Senior Member, IEEE), YANTAO LI^{ID}1,4, AND LAN JIANG^{ID}1,5

¹College of Electrical Engineering and New Energy, China Three Gorges University, Yichang 443002, China

²Discipline of Electrical and Computer Engineering, Curtin University, Perth, WA 6102, Australia

³Hubei Provincial Key Laboratory of Operation and Control of Cascade Hydropower Stations, Yichang 443002, China

⁴Hubei Provincial Yi Ling District Power Supply Company, Yichang 443100, China

⁵College of Civil Engineering, Hunan University, Changsha 410000, China

Corresponding author: Lan Jiang (jianglan@hnu.edu.cn).

This work was supported by the National Natural Science Foundation of China under Grant 51877122 and Grant 51707104.

ABSTRACT In the conventional electromagnetic tube expansion, axial distribution of the electromagnetic force is not uniform along the workpiece. This results in uneven axial deformation of the deformed tube and restricts the full industrial implementation of this technology. In an attempt to overcome this issue, this article proposes a new method based on dual-coil electromagnetic tube compression. In this regard, an electromagnetic-structure finite element coupling model is developed to emulate the real electromagnetic tube compression process. Influence of the proposed dual-coil structure parameters on the electromagnetic force distribution is analyzed. Results show that the proposed dual-coil electromagnetic tube compression method can effectively solve the problem of uneven axial deformation in the conventional electromagnetic tube compression. The proposed method is expected to promote wide industrial applications of the electromagnetic tube forming technology.

INDEX TERMS Electromagnetic forming, electromagnetic tube compression, axial uneven deformation, dual-coil, electromagnetic force distribution.

I. INTRODUCTION

In view of the urgent need for future sustainable and environmentally-friendly products, recyclable lightweight materials play an important role in modern advanced manufacturing technology and structural design [1]–[3]. Compared with the traditional mechanical forming, electromagnetic forming (EMF) features improved stress distribution [4]–[6], reduced wrinkling [7]–[9] and increased forming limit [10]–[12]. Due to these advantageous, EMF is widely used in aerospace and automobile industry [13], [14] to process light alloy materials such as aluminum [15] and titanium [16].

In general, EMF can be categorized into electromagnetic tube compression [17]–[19] and electromagnetic tube expansion [20]–[22]. Due to the end effect of the uneven

electromagnetic force distribution [23], [3], both the electromagnetic tube compression and the electromagnetic tube expansion exhibit non-uniform axial deformation [24]. Some techniques have been suggested and published in the literature to overcome this issue. For instance, Qiu *et al.* [25] proposed the use of a concave driving coil to improve the tube axial deformation uniformity through weakening the radial electromagnetic force at the middle section of the tube. Both simulation and experimental results revealed good tube deformation performance. The tube electromagnetic compression also exhibits the phenomenon of wrinkling. As such, Savadkoohian *et al.* [26] studied the influence of the discharge voltage, tube thickness and radius of mold on the tube wrinkling using analytical energy method. Bartels *et al.* [27] established a sequential coupling model for electromagnetic tube compression. Daehn *et al.* [28] conducted an experimental study on electromagnetic tube compression and the reported results showed a negligible wrinkling of pipe fittings

The associate editor coordinating the review of this manuscript and approving it for publication was Mehmet Alper Uslu.

can be achieved when the outer diameter compression rate is less than 5%. In addition, Yu and Chun-Feng [29] found that the axial deformation uniformity of an electromagnetic tube compression is significantly correlated to the length of the tube and driving coil.

In order to further explore effective solutions to the problem of axial deformation uniformity in electromagnetic tube compression, this article proposes a new dual-coil electromagnetic tube compression method. Based on the electromagnetic structure coupling model, the electromagnetic force distribution and the axial deformation uniformity are analyzed when the proposed method is employed.

II. BASIC PRINCIPLE OF EMF

A. TRADITIONAL ELECTROMAGNETIC TUBE COMPRESSION

In the conventional method, the driving coil is placed outside the tube. The capacitor power supply generates a pulsed current within the coil which generates a magnetic field and at the same time, an induced eddy current on the tube. The interaction between the magnetic field and the induced eddy current produces a pulsed electromagnetic force that drives the tube deformation.

The electromagnetic force density acting on the tube during the forming process can be calculated from:

$$F = J_e \times B \quad (1)$$

where, B is the magnetic flux density and J_e is the induced eddy current density.

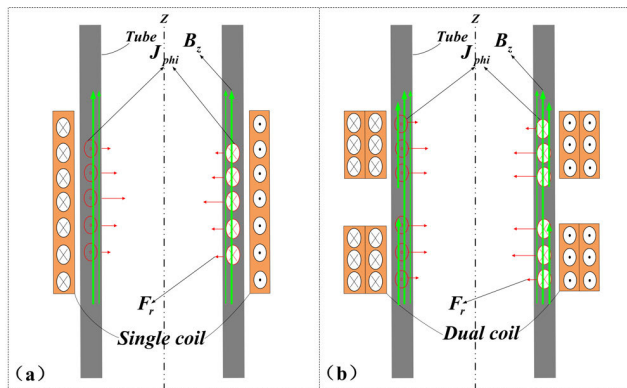


FIGURE 1. Schematic of the Electromagnetic forming setup. (a) Conventional single coil topology, (b) proposed dual-coil topology.

Due to the axisymmetric structure of the system, only the circumferential component of the induced current density J_{phi} exists. Figure 1(a) shows a schematic diagram of the traditional electromagnetic tube compression setup. The electromagnetic force density F can be divided into radial F_r and axial F_z components that can be calculated from:

$$F_r = J_{phi} \cdot B_z \quad (2)$$

$$F_z = J_{phi} \cdot B_r \quad (3)$$

During the electromagnetic tube compression process, the load of the tube is mainly radial electromagnetic force, which is determined by the circumferential induced eddy current density and the axial magnetic flux density B_z . Due to the tube end effect, the axial magnetic flux density in the middle part of the tube is larger than that at both tube ends. As a result, the radial electromagnetic force at both ends of the tube is less than the force in the middle part which leads to uneven axial tube deformation.

B. PROPOSED DUAL-COIL ELECTROMAGNETIC TUBE COMPRESSION

In order to improve the uniformity of axial deformation in the tube electromagnetic compression process, a feasible solution is to weaken the radial electromagnetic force exerted on the middle region of the tube. To achieve this, Figure 1(b) shows the basic principle of the proposed method. As can be seen in the figure, the single coil, used in the conventional EMF, is replaced by two separate driving coils placed in the axial direction of the workpiece. Hence, the radial electromagnetic force loading on the middle of the tube can be effectively reduced which results in improved tube axial deformation uniformity. For comparability, the length of the two driving coils along with the space between them is assumed to be the same length of the conventional single coil in Figure 1(a).

According to the superposition principle, the electromagnetic force density F of the two coils becomes

$$F = (J_1 + J_2) \times (B_1 + B_2 + B_0) \quad (4)$$

where, J_1 and J_2 are respectively the induced eddy current densities generated by the two driving coils on the tube. B_1 and B_2 are respectively the magnetic flux densities generated by the two coils, and B_0 is the self-induced magnetic flux density of the tube.

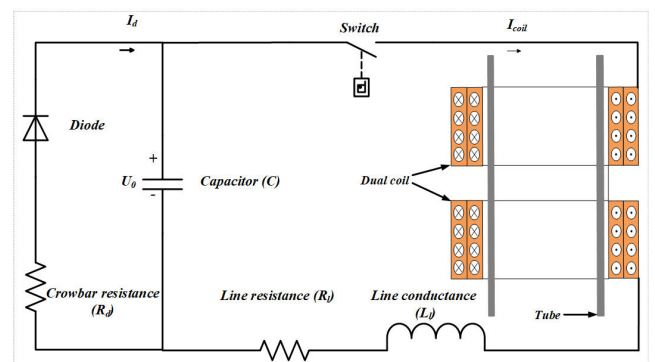


FIGURE 2. Schematic diagram of the electromagnetic tube compression system.

In order to extend the operational life of the driving coil, a crowbar branch is added to the circuit as shown in Figure 2. In the proposed model shown in Figure 2, the upper and lower coils are connected in series in the same direction. The parameters of this circuit are listed in Table 1. According to Kirchhoff's law, the current of the driving coils can be

TABLE 1. Parameters of the model circuit and tube.

| Parameter | Description | Value |
|-----------------------|-------------------------|--------------------------------|
| circuit | | |
| C | Discharge capacitance | 320 μF |
| L_l | Line inductance | 12 μH |
| R_l | Line resistance | 0.005 Ω |
| R_d | Crowbar resistance | 0.02 Ω |
| Tube(AA6061-O) | | |
| ρ | Density | 2700 kg/m^3 |
| γ | Electrical conductivity | $3.03 \times 10^7 \text{ S/m}$ |
| σ_s | Initial yield stress | 32.6 MPa |
| μ | Poisson's ratio | 0.33 |
| E | Young's modulus | 70 GPa |

calculated from:

$$(R_l \vec{I}_l + L_l \frac{d\vec{I}_l}{dt}) + (R_{c1} + R_{c2}) \vec{I}_l \quad (5)$$

$$+ (L_{c1} + L_{c2} + 2M) \frac{d\vec{I}_l}{dt} + (M_1 + M_2) \frac{d\vec{I}_w}{dt} = \vec{U}_c$$

$$R_w \vec{I}_w + L_w \frac{d\vec{I}_w}{dt} + (M_1 + M_2) \frac{d\vec{I}_l}{dt} = 0 \quad (6)$$

$$\vec{U}_c = \vec{U}_0 - \frac{1}{C} \int_0^t (\vec{I}_l + \vec{I}_d) dt \quad (7)$$

$$\begin{cases} \vec{I}_d = 0 & (U_c \geq 0) \\ \vec{I}_d = \frac{\vec{U}_c}{R_d} & (U_c < 0) \end{cases} \quad (8)$$

$$\vec{I}_c = \vec{I}_l + \vec{I}_d \quad (9)$$

where, M_1 is the mutual inductance between the upper coil and tube, M_2 is the mutual inductance between the lower coil and tube, M is the mutual inductance between the two coils. R_c and L_c are respectively the equivalent resistance and equivalent inductance of the two coils, \vec{I}_c is the capacitive current, \vec{I}_l is the coil current, \vec{I}_d is the crowbar current, \vec{I}_w is the induced eddy current in the tube.

III. ELECTROMAGNETIC-STRUCTURAL COUPLING MODEL

Ignoring the effect of temperature, the process of the electromagnetic tube compression can be regarded as a dynamic coupling process of electromagnetic field with structure field. Also, based on [28], the tube wrinkle is negligible when the radial compression of the tube's outer diameter is less than 5%. Based on these two points, the proposed model can be simplified into a two-position axisymmetric model that can be simulated using COMSOL multiphysical software as shown in Figure 3. The workpiece adopted in this article is an aluminum alloy (AA6061-O) with a thickness of 2 mm, 79 mm outer diameter and a length of 120 mm. The initial structural dimensions of the conventional and proposed systems are shown in Figure 3.

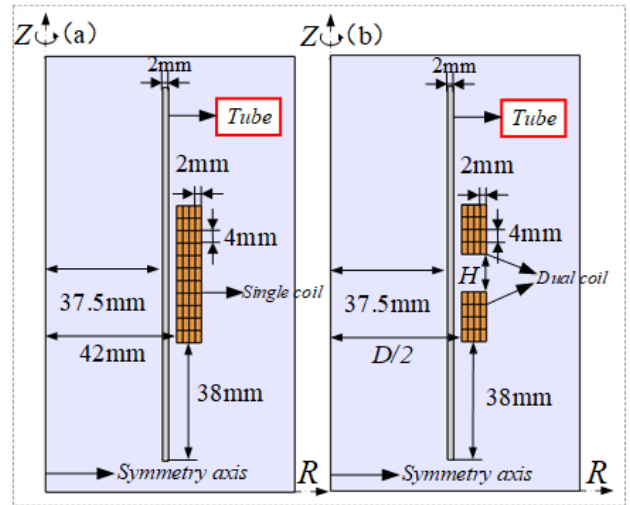


FIGURE 3. Geometric dimensions. (a) Conventional single coil topology, (b) proposed dual-coil topology.

A. ELECTROMAGNETIC MODEL

The electromagnetic model is used to calculate the electromagnetic force acting on the tube, which is then applied as a load to the structure model to simulate the tube deformation.

According to Maxwell's equations, the magnetic potential vector \mathbf{A} in the electromagnetic model can be expressed as:

$$\nabla \times \left(\frac{1}{\mu} \nabla \times \mathbf{A} \right) + \gamma \frac{\partial \mathbf{A}}{\partial t} = \mathbf{J} \quad (10)$$

where \mathbf{J}_e represents the induced eddy current, μ is the magnetic permeability of the tube material, while γ is the conductivity of the material.

The expressions of the magnetic potential vectors for different areas can be expressed as below.

Air gap area:

$$\nabla \times \left(\frac{1}{\mu} \nabla \times \mathbf{A} \right) = 0 \quad (11)$$

Coil area:

$$\nabla \times \left(\frac{1}{\mu} \nabla \times \mathbf{A} \right) = \mathbf{J} \quad (12)$$

Tube area:

$$\nabla \times \left(\frac{1}{\mu} \nabla \times \mathbf{A} \right) = -\gamma \frac{\partial \mathbf{A}}{\partial t} \quad (13)$$

The electromagnetic force density of the tube can be expressed as:

$$\mathbf{F} = \nabla \times \left(\frac{1}{\mu} \nabla \times \mathbf{B} \right) \times \mathbf{B} = \mathbf{J} \times \mathbf{B} \quad (14)$$

B. STRUCTURAL MODEL

The electromagnetic force density is the load force of the tube. The transient dynamic balance equation and Newmark

time integral method are used to identify this force as below.

$$M \frac{\partial^2 \mathbf{u}}{\partial t^2} + C \frac{\partial \mathbf{u}}{\partial t} + K \mathbf{u} = \mathbf{F}^a \quad (15)$$

where, M is the structure mass matrix, C is the structure damping matrix, K is the structure stiffness matrix, \mathbf{F} is the load vector, \mathbf{u} is the node displacement vector.

According to Suzuki [30], the flow stress of the tube is approximately calculated as follows:

$$\sigma = k(\alpha + \varepsilon^P)^n \quad (16)$$

$$\alpha = (\sigma_{ys0}/k)^{\frac{1}{n}} \quad (17)$$

where, k is the strength coefficient, n is the hardening coefficient, σ_{ys0} is the initial yield stress, ε is the plastic strain; other parameters of the tube are listed in Table 1.

The authors of this article used this electromagnetic-structural model to study the electromagnetic tube bulging using a concave coil [20]. Simulation results were in good agreement with the experimental data, as shown in Figure 4. So, this model is reliable and can be effectively used to study the distribution of the electromagnetic force and axial deformation uniformity during the process of tube compression.

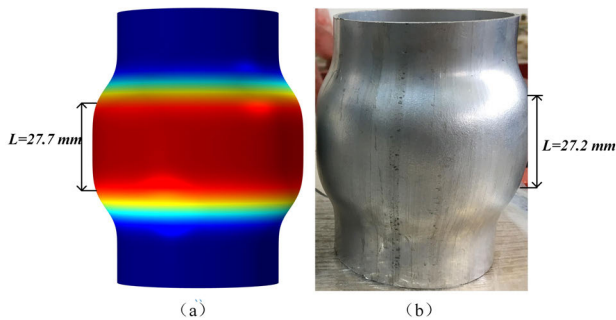


FIGURE 4. Simulation and experimental results of the electromagnetic tube bulging based on concave coil reported in [20].

IV. ANALYSIS OF RADIAL ELECTROMAGNETIC FORCE AND AXIAL UNIFORMITY

The axial distribution of the radial electromagnetic force plays a significant role in the axial uniformity improvement of the tube compression process. This section investigates the effect of two structural parameters; gap length between the two coils H and the coil inner diameter D on the radial electromagnetic force and axial deformation uniformity. The gap between the two coils influences their axial position while the inner diameter dominates their radial position with respect to the workpiece. It is worth mentioning that other coil parameters such as number of turns and coil length also affect the radial electromagnetic force and the tube axial uniformity. However, these parameters are kept constant in this article for accurate comparison of the proposed and conventional EMF methods.

A. EFFECT OF H ON THE RADIAL ELECTROMAGNETIC FORCE AND AXIAL DEFORMATION UNIFORMITY

As shown in Figure 3(b), the initial coil parameters are: gap length $H=12$ mm, inner diameter $D=84$ mm, and outer

diameter is 100mm. In order to investigate the influence of different coil structure parameters on the electromagnetic tube compression, the method of single parameter variation is adopted to study the influence of the gap length H and inner diameter D on the radial electromagnetic force and axial deformation uniformity. The gap length is varied in the range $H=8\sim 20$ mm while the range of the inner diameter is assumed to be $D=81\sim 85$ mm. In all studied cases, the amplitude of the current density of the dual-coil system is set at $4.55 \times 10^8 A/m^2$. When either H or D is varied within the above-mentioned range, the other parameter is maintained at the initial value mentioned above.

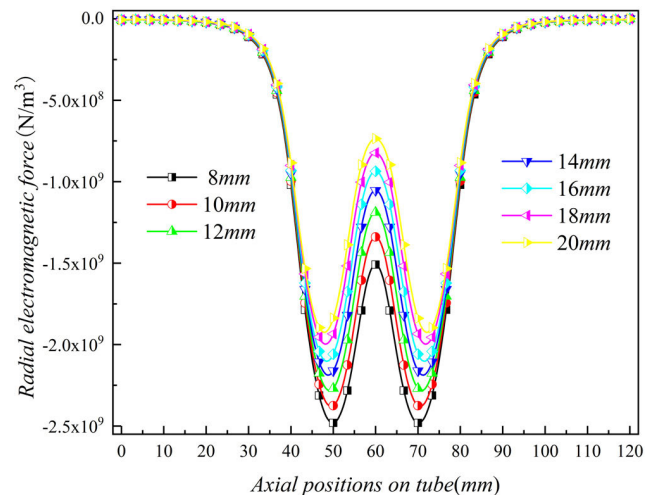


FIGURE 5. The effect of H (gap length) on the radial electromagnetic force.

Figure 5 shows the effect of H on the radial electromagnetic force. Because of the two separate coils, the radial electromagnetic force profile comprises two peaks located between the middle of the tube and its two ends. With the increase of H , the two peak points gradually move toward the ends of the tube while the force on the middle part is decreasing.

Figure 6 shows the influence of the gap length H on the axial deformation uniformity. When the two peaks of the radial electromagnetic force are close to the middle of the tube, the tube axial deformation is of convex profile. By increasing H , the two peaks of the radial electromagnetic force become closer to the tube ends and the axial deformation profile becomes concave. Obviously, there is a critical value of H at which the axial compression deformation profile converts from convex to concave. In this example, when the gap length H reaches a critical value of about 12 mm, a uniform axial deformation of the tube can be realized as shown in Figure 6.

B. EFFECT OF D ON THE RADIAL ELECTROMAGNETIC FORCE AND AXIAL DEFORMATION UNIFORMITY

Figure 7 shows the effect of the inner diameter D on the radial electromagnetic force. It can be observed that when the

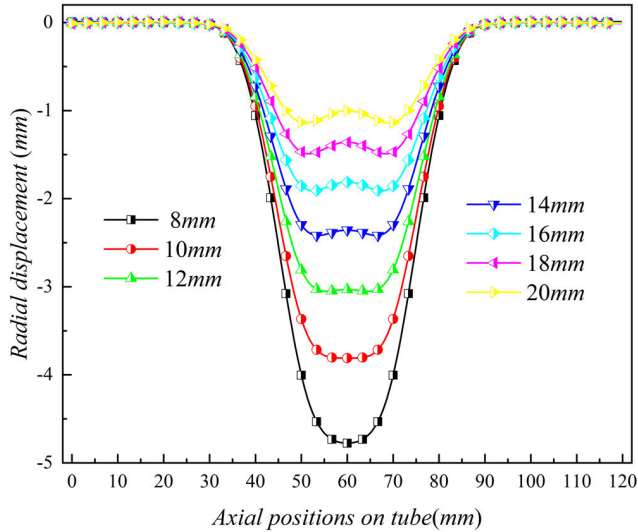


FIGURE 6. The effect of H (gap length) on the axial deformation uniformity.

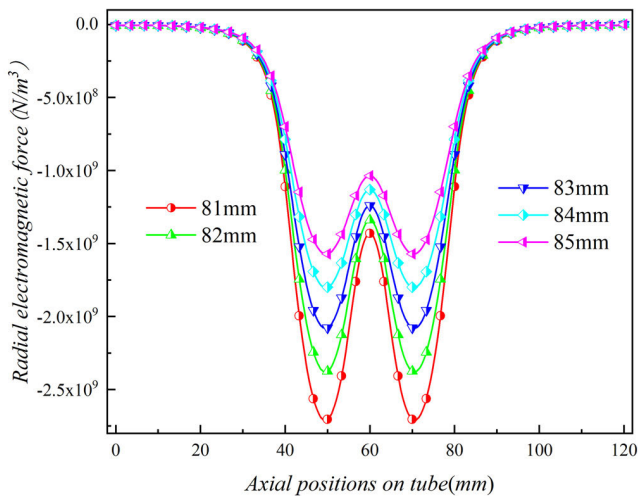


FIGURE 7. The effect of D (inner diameter) on the radial electromagnetic force.

inner diameter increases, the two peaks of the radial electromagnetic force don't change in the axial position, while the difference between the two peaks along with the radial electromagnetic force at the center of the tube become smaller. Figure 8 shows the effect of D on the axial deformation uniformity. With the variation of D , the difference between the two peak positions and the value of the radial electromagnetic force at the center of the tube are also adjusted. At a particular value of D , the deformation of the tube in the axial direction becomes relatively uniform. In this example, the critical value of D is 82mm.

The above analysis shows that the electromagnetic tube compression based on dual-coil can improve the distribution of the radial electromagnetic force, so as to improve the axial deformation uniformity of the tube.

V. COMPARISON WITH THE CONVENTIONAL METHOD

In order to attest the robustness of the proposed method, the radial electromagnetic force and axial uniformity are com-

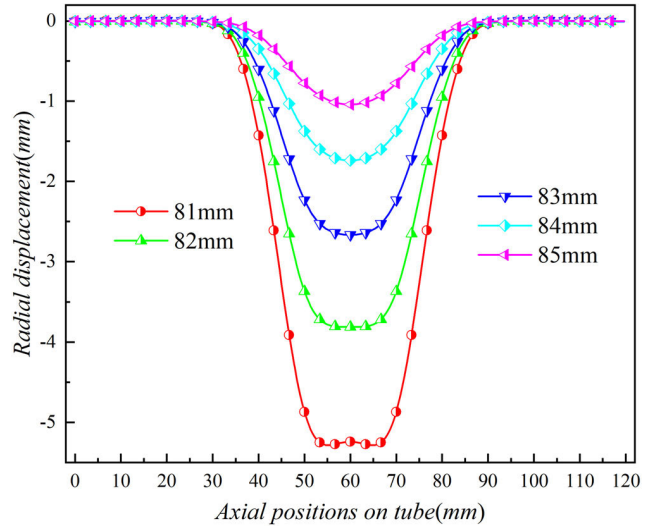


FIGURE 8. The effect of D (inner diameter) on the axial deformation uniformity.

TABLE 2. Coils parameters of the investigated two systems.

| unit: mm | Height | Inner diameter | Outer diameter |
|-------------|--------|----------------|----------------|
| Single coil | 44 | 84 | 100 |
| Dual-coil | upper | 16 | 84 |
| | lower | 16 | 84 |

pared for two different systems; conventional single coil and the proposed two coils based on the data shown in Table 2. For enhancing the comparability of the simulation results, the maximum deformation of the two systems is set at 3.6mm. So, the discharge voltage of the single and dual-coil are respectively set to 1.87kV and 2.34kV.

It is worth noting that the discharge voltage is to be increased by 0.47kV than the single coil method in order to achieve the same maximum deformation using the proposed method. This voltage increment does not increase the discharge energy significantly as the generated pulsed current is of short duration.

Figure 9 shows the distribution of the radial electromagnetic force density when the two above systems are employed. With the traditional single coil system, the radial electromagnetic force has one peak that is axially located on the middle of the tube. In case of the proposed dual-coil system, the radial electromagnetic force comprises two peaks that are axially located on the two sides of the tube with a reduction of the force exerted on the middle part, hence more tube deformation uniformity can be attained. Figure 10 shows the deformation profile of the tube when loaded with the two investigated systems. As can be observed, compared with the traditional single coil electromagnetic tube compression system, the proposed dual-coil electromagnetic tube compression system exhibits improved axial uniformity.

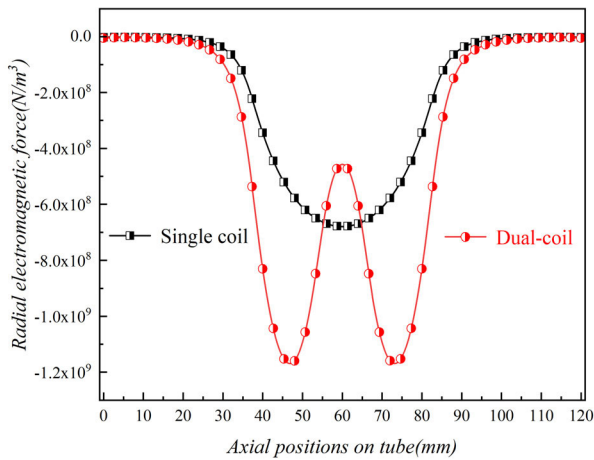


FIGURE 9. Radial electromagnetic force distribution under the investigated two systems.

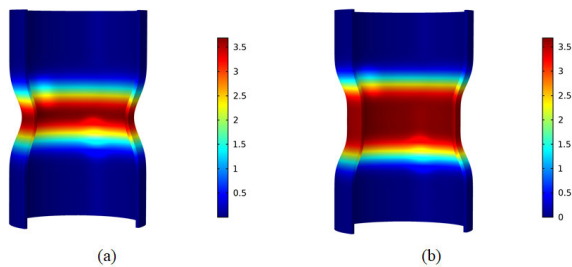


FIGURE 10. Deformation profile of the tube. (a) Conventional single coil topology, (b) proposed dual-coil topology.

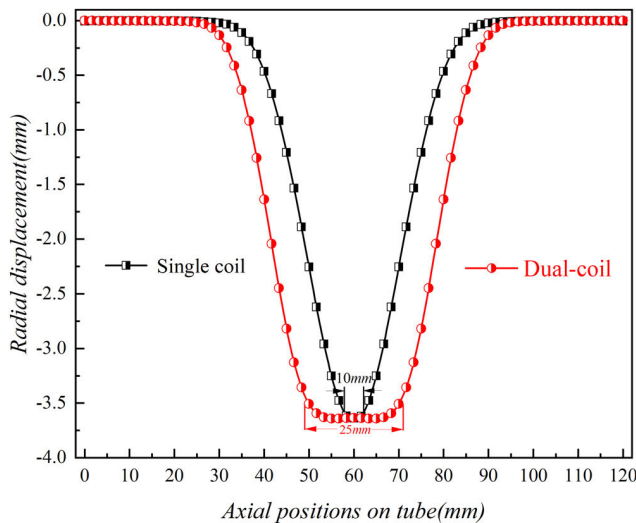


FIGURE 11. Deformation profile of the tube for conventional single coil topology and the proposed dual-coil topology.

To quantify the tube uniformity, a compression uniformity coefficient D_r is introduced. D_r is defined as the axial length when the radial compression of the pipe is greater than 90% of the maximum displacement. Figure. 11 shows the radial compression displacement of the tube with the two investigated driving systems. Under traditional single coil system, D_r is 10mm. On the other hand, D_r increases to 25mm under dual-coil system; indicating the axial deformation uniformity

is improved 2.5 times compared to the conventional method. These results prove the capability of the proposed dual-coil topology to improve the axial deformation uniformity and thus overcoming one of the main issues of the conventional EMF based on single coil topology.

VI. CONCLUSION

In order to solve the problem of the non-uniform axial deformation in conventional EMF, this article proposes a new EMF method based on dual-coil topology, which can provide a reasonable radial electromagnetic force on the deformed tube. Results show that optimum adjustment of the gap length can change the position of the two peak points of the radial electromagnetic force acting on the tube in the axial direction. Similarly, the inner diameter of the coil influences the difference between the two peak points and the center point of the tube. Hence, the compression deformation in the axial direction of the tube exhibits a profile that changes from convex to concave at optimum values of the gap length and the tube inner diameter. In other words, there exists a reasonable coil structure that makes the axial deformation uniformity of the tube optimal. Results prove that the proposed dual-coil electromagnetic tube compression method can effectively solve the problem of uneven axial deformation exists in the conventional EMF method. Further analysis on other coil parameters such as number of turns, coil length along with experimental validation is to be carried out to promote the feasibility of the method proposed in this article.

REFERENCES

- [1] Q. Cao, L. Du, Z. Li, Z. Lai, Z. Li, M. Chen, X. Li, S. Xu, Q. Chen, X. Han, and L. Li, "Investigation of the Lorentz-force-driven sheet metal stamping process for cylindrical cup forming," *J. Mater. Process. Technol.*, vol. 271, pp. 532–541, Sep. 2019.
- [2] L. Qiu, B. Wang, A. Abu-Siada, Q. Xiong, W. Zhang, W. Ge, C. Liu, L. Jiang, and C. Wang, "Research on forming efficiency in double-sheet electromagnetic forming process," *IEEE Access*, vol. 8, pp. 19248–19255, 2020.
- [3] X. Zhang, Q. Cao, X. Han, Q. Chen, Z. Lai, Q. Xiong, F. Deng, and L. Li, "Application of triple-coil system for improving deformation depth of tube in electromagnetic forming," *IEEE Trans. Appl. Supercond.*, vol. 26, no. 4, pp. 1–4, Jun. 2016.
- [4] W. Luo, L. Huang, J. Li, X. Liu, and Z. Wang, "A novel multi-layer coil for a large and thick-walled component by electromagnetic forming," *J. Mater. Process. Technol.*, vol. 214, no. 11, pp. 2811–2819, Nov. 2014.
- [5] L. Qiu, N. Yi, A. Abu-Siada, J. Tian, Y. Fan, K. Deng, Q. Xiong, and J. Jiang, "Electromagnetic force distribution and forming performance in electromagnetic forming with discretely driven rings," *IEEE Access*, vol. 8, pp. 16166–16173, 2020.
- [6] Q. Cao, Z. Li, Z. Lai, Z. Li, X. Han, and L. Li, "Analysis of the effect of an electrically conductive die on electromagnetic sheet metal forming process using the finite element-circuit coupled method," *Int. J. Adv. Manuf. Technol.*, vol. 101, nos. 1–4, pp. 549–563, Mar. 2019.
- [7] L. Qiu, K. Deng, Y. Li, X. Tian, Q. Xiong, P. Chang, P. Su, and L. Huang, "Analysis of coil temperature rise in electromagnetic forming with coupled cooling method," *Int. J. Appl. Electromagn. Mech.*, vol. 63, no. 1, pp. 45–58, May 2020, doi: 10.3233/JAE-190062.
- [8] N. Liu, Z. Lai, Q. Cao, L. Li, X. Han, Y. Huang, M. Chen, X. Li, and Y. Lv, "Investigation of accurate forming of a semi-ellipsoidal shell part by an electromagnetic forming method," *Int. J. Adv. Manuf. Technol.*, vol. 105, nos. 1–4, pp. 1113–1128, Nov. 2019.

- [9] L. Qiu, W. Zhang, A. Abu-Siada, G. Liu, C. Wang, Y. Wang, B. Wang, Y. Li, and Y. Yu, "Analysis of electromagnetic force and formability of tube electromagnetic bulging based on convex coil," *IEEE Access*, vol. 8, pp. 33215–33222, 2020.
- [10] Q. Cao, Z. Lai, Q. Xiong, Q. Chen, T. Ding, X. Han, and L. Li, "Electromagnetic attractive forming of sheet metals by means of a dual-frequency discharge current: Design and implementation," *Int. J. Adv. Manuf. Technol.*, vol. 90, nos. 1–4, pp. 309–316, Apr. 2017.
- [11] L. Qiu, K. Deng, A. Abu-Siada, Q. Xiong, N. Yi, Y. Fan, J. Tian, and J. Jiang, "Construction and analysis of two-dimensional axisymmetric model of electromagnetic tube bulging with field shaper," *IEEE Access*, vol. 8, pp. 113713–113719, 2020.
- [12] H. Yu, Q. Zheng, S. Wang, and Y. Wang, "The deformation mechanism of circular hole flanging by magnetic pulse forming," *J. Mater. Process. Technol.*, vol. 257, pp. 54–64, Jul. 2018.
- [13] L. Qiu, C. Wang, A. Abu-Siada, Q. Xiong, W. Zhang, B. Wang, N. Yi, Y. Li, and Q. Cao, "Coil temperature rise and workpiece forming efficiency of electromagnetic forming based on half-wave current method," *IEEE Access*, vol. 8, pp. 9371–9379, 2020.
- [14] S. Ouyang, X. Li, C. Li, L. Du, T. Peng, X. Han, L. Li, Z. Lai, and Q. Cao, "Investigation of the electromagnetic attractive forming utilizing a dual-coil system for tube bulging," *J. Manuf. Process.*, vol. 49, pp. 102–115, Jan. 2020.
- [15] L. Qiu, Y. Li, Y. Yu, Y. Xiao, P. Su, Q. Xiong, J. Jiang, and L. Li, "Numerical and experimental investigation in electromagnetic tube expansion with axial compression," *Int. J. Adv. Manuf. Technol.*, vol. 104, nos. 5–8, pp. 3045–3051, Oct. 2019.
- [16] Q. Cao, X. Han, Z. Lai, Q. Xiong, X. Zhang, Q. Chen, H. Xiao, and L. Li, "Analysis and reduction of coil temperature rise in electromagnetic forming," *J. Mater. Process. Technol.*, vol. 225, pp. 185–194, Nov. 2015.
- [17] H.-P. Yu, C.-F. Li, D.-H. Liu, and X. Mei, "Tendency of homogeneous radial deformation during electromagnetic compression of aluminium tube," *Trans. Nonferrous Met. Soc. China*, vol. 20, no. 1, pp. 7–13, Jan. 2010.
- [18] L. Qiu, Y. Li, Y. Yu, A. Abu-Siada, Q. Xiong, X. Li, L. Li, P. Su, and Q. Cao, "Electromagnetic force distribution and deformation homogeneity of electromagnetic tube expansion with a new concave coil structure," *IEEE Access*, vol. 7, pp. 117107–117114, 2019.
- [19] L. Huang, J. Zhang, J. Zou, Y. Zhou, and L. Qiu, "Effect of equivalent radius of drive coil on forming depth in electromagnetic sheet free bulging," *Int. J. Appl. Electromagn. Mech.*, vol. 61, no. 3, pp. 377–389, Nov. 2019.
- [20] L. Qiu, Y. Yu, Z. Wang, Y. Yang, Y. Yang, and P. Su, "Analysis of electromagnetic force and deformation behavior in electromagnetic forming with different coil systems," *Int. J. Appl. Electromagn. Mech.*, vol. 57, no. 3, pp. 337–345, Jun. 2018.
- [21] L. Qiu, K. Deng, X. Yang, A. Abu-Siada, Q. Xiong, N. Yi, J. Jiang, and L. Xiao, "Electromagnetic force distribution and forming performance in electromagnetic tube expansion with axial compression," *IEEE Access*, vol. 8, pp. 134514–134523, 2020, doi: 10.1109/ACCESS.2020.3010552.
- [22] F.-Q. Li, Y. Fang, Y. Zhu, J.-H. Mo, and J.-J. Li, "Study on the homogeneity of deformation under electromagnetic expansion of metal tube," *Int. J. Appl. Electromagn. Mech.*, vol. 42, no. 1, pp. 13–25, Feb. 2013.
- [23] L. Qiu, W. Zhang, A. Abu-Siada, Q. Xiong, C. Wang, Y. Xiao, B. Wang, Y. Li, J. Jiang, and Q. Cao, "Electromagnetic force distribution and wall thickness reduction of three-coil electromagnetic tube bulging with axial compression," *IEEE Access*, vol. 8, pp. 21665–21675, 2020.
- [24] J.-J. Yan, M.-T. Chen, W.-M. Quach, M. Yan, and B. Young, "Mechanical properties and cross-sectional behavior of additively manufactured high strength steel tubular sections," *Thin-Walled Struct.*, vol. 144, Nov. 2019, Art. no. 106158.
- [25] L. Qiu, Y. Yu, Q. Xiong, C. Deng, Q. Cao, X. Han, and L. Li, "Analysis of electromagnetic force and deformation behavior in electromagnetic tube expansion with concave coil based on finite element method," *IEEE Trans. Appl. Supercond.*, vol. 28, no. 3, Apr. 2018, Art. no. 0600705.
- [26] H. Savadkoohian, A. A. Fallahi, and B. Arezoo, "Analytical and experimental study of wrinkling in electromagnetic tube compression," *Int. J. Adv. Manuf. Technol.*, vol. 93, pp. 901–914, May 2017.
- [27] G. Bartels, W. Schätzing, H.-P. Scheibe, and M. Leone, "Comparison of two different simulation algorithms for the electromagnetic tube compression," *Int. J. Mater. Forming*, vol. 2, no. S1, pp. 693–696, Aug. 2009.
- [28] A. Vivek, K.-H. Kim, and G. S. Daehn, "Simulation and instrumentation of electromagnetic compression of steel tubes," *J. Mater. Process. Technol.*, vol. 211, no. 5, pp. 840–850, May 2011.
- [29] Y.-U. Yu and L. I. Chun-Feng, "Effects of coil length on tube compression in electromagnetic forming," *Trans. Nonferrous Metals Soc. China*, vol. 17, no. 6, pp. 1270–1275, 2007.
- [30] H. Suzuki, H. Negishi, Y. Yokouchi, and M. Murata, "Free expansion of tube under magnetic pressure," *J. Jpn. Soc. Technol. Plasticity*, vol. 310, no. 27, pp. 1254–1260, 1986.



LI QIU (Member, IEEE) received the B.S., M.S., and Ph.D. degrees in electrical engineering from the Huazhong University of Science and Technology, Wuhan, China, in 2012. He is currently an Associate Professor with the College of Electrical Engineering and New Energy, China Three Gorges University, Yichang. He is the author of more than 15 articles and more than ten inventions. His research interests include the technology of pulsed high-magnetic field, high-voltage technology, and electromagnetic forming. He is a Periodical Reviewer of the IEEE TRANSACTIONS ON APPLIED SUPERCONDUCTIVITY and the *International Journal of Applied Electromagnetics and Mechanics*.

YUDONG WANG was born in Hubei, China, in 1995. He received the bachelor's degree from the College of Electrical Engineering and New Energy, China Three Gorges University, Yichang, where he is currently a Graduate Student in electrical engineering.

ZHANG WANG is currently a Graduate Student in control science and engineering with the College of Electrical Engineering and New Energy, China Three Gorges University, Yichang.



AHMED ABU-SIADA (Senior Member, IEEE) received the B.Sc. and M.Sc. degrees in electrical engineering from Ain Shams University, Egypt, in 1998, and the Ph.D. degree from Curtin University, Australia, in 2004. He is currently an Associate Professor and a Discipline Lead of the Electrical and Computer Engineering, Curtin University. His research interests include power electronics, power system stability, condition monitoring, and power quality. He is the Editor-in-Chief of the *International Journal of Electrical and Electronic Engineering* and a Regular Reviewer for various IEEE TRANSACTIONS. He is a Vice-Chair of the IEEE Computation Intelligence Society and WA Chapter.

Chief of the *International Journal of Electrical and Electronic Engineering* and a Regular Reviewer for various IEEE TRANSACTIONS. He is a Vice-Chair of the IEEE Computation Intelligence Society and WA Chapter.

YANTAO LI is currently pursuing the degree with State Grid Yiling Power Supply Company, Yichang, Hubei, China.



LAN JIANG was born in Hubei, China, in 1986. He received the master's degree from the College of Civil Engineering, Guizhou University, Guiyang, China, in 2012. He is currently pursuing the Ph.D. degree in civil engineering with Hunan University, Changsha, China. His research interests include disaster prevention and mitigation and optimization design of power engineering structure, and dynamic performance of engineering structures.

•••